Quantifying the Ion Selectivity of the Ca^{2+} Site in Photosystem II: Evidence for Direct Involvement of Ca^{2+} in O_2 Formation†

John S. Vrettos, Daniel A. Stone,‡ and Gary W. Brudvig*

Department of Chemistry, Yale University, New Haven, Connecticut 06520-8107

Received April 4, 2001; Revised Manuscript Received May 10, 2001

ABSTRACT: Calcium is an essential cofactor in the oxygen-evolving complex (OEC) of photosystem II (PSII). The removal of Ca^{2+} or its substitution by any metal ion except Sr^{2+} inhibits oxygen evolution. We used steady-state enzyme kinetics to measure the rate of O_2 evolution in PSII samples treated with an extensive series of mono-, di-, and trivalent metal ions in order to determine the basis for the affinity of metal ions for the Ca^{2+}-binding site. Our results show that the Ca^{2+}-binding site in PSII behaves very similarly to the Ca^{2+}-binding sites in other proteins, and we discuss the implications this has for the structure of the site in PSII. Activity measurements as a function of time show that the binding site achieves equilibrium in 4 h for all of the PSII samples investigated. The binding affinities of the metal ions are modulated by the 17 and 23 kDa extrinsic polypeptides; their removal decreases the free energy of binding of the metal ions by 2.5 kcal/mol, but does not significantly change the time required to reach equilibrium. Monovalent ions are effectively excluded from the Ca^{2+}-binding site, exhibiting no inhibition of O_2 evolution. Di- and trivalent metal ions with ionic radii similar to that of Ca^{2+} (0.99 Å) bind competitively with Ca^{2+} and have the highest binding affinity, while smaller metal ions bind more weakly and much larger ones do not bind competitively. This is consistent with a size-selective Ca^{2+}-binding site that has a rigid array of coordinating ligands. Despite the large number of metal ions that competitively replace Ca^{2+} in the OEC, only Sr^{2+} is capable of partially restoring activity. Comparing the physical characteristics of the metal ions studied, we identify the pK_a of the aqua ion as the factor that determines the functional competence of the metal ion. This suggests that Ca^{2+} is directly involved in the chemistry of water oxidation and is not only a structural cofactor in the OEC. We propose that the role of Ca^{2+} is to act as a Lewis acid, binding a substrate water molecule and tuning its reactivity.

The light-driven oxidation of water is catalyzed by photosystem II (PSII)[1] at the OEC, which consists of a Mn_4 cluster, Y_Z, and Cl^- and Ca^{2+} cofactors. Upon absorption of a photon, the reaction center Chl, P680, donates an electron to a membrane-bound quinone, Q_A. $P680^+$ is reduced by Y_Z, which in turn oxidizes the Mn_4 cluster. The Mn_4 cluster is oxidized through a series of five 'S_n states' ($n = 0-4$), where S_0 is the most reduced state. Upon formation of the S_4 state, the Mn_4 cluster is reduced by four electrons to S_0 by oxidizing H_2O to O_2 and four protons [for reviews, see (*1*−*4*)].

Ca^{2+} is required for water oxidation (*5*, *6*); its depletion from PSII results in inhibition of the S-state cycle (*7*, *8*). The requirement for Ca^{2+} and the involvement of the 17 and 23 kDa extrinsic polypeptides in binding Ca^{2+} were shown by washing PSII samples with 1−2 M NaCl (*9*−*11*). This treatment removes the 17 and 23 kDa extrinsic polypeptides and causes Ca^{2+} to be released from the protein. Activity can be restored to NaCl-treated PSII by rebinding the 17 and 23 kDa extrinsic polypeptides in the presence of low concentrations of Ca^{2+} or by incubating the sample with millimolar concentrations of Ca^{2+} for extended periods of time. That the extrinsic polypeptides need to be removed in order for Ca^{2+} to be released, but are not required for the restoration of activity, led to the proposal that the extrinsic polypeptides serve as a diffusion barrier, sequestering Ca^{2+} within the protein and preventing it from equilibrating with Ca^{2+} in the bulk medium (*9*).

Many techniques have been applied to study the number of Ca^{2+}-binding sites in PSII and their affinities, including steady-state activity measurements (*12*), atomic absorption (*13*), scintillation counting using $^{45}Ca^{2+}$ (*14*), and equilibrium measurements employing a Ca^{2+}-sensitive electrode (*15*). One difficulty with interpreting the results obtained by all but the last method is that the measurements of Ca^{2+} binding are not made at equilibrium, as these methods require the

† This work was supported by National Institutes of Health Grant GM32715.

* Corresponding author. Phone: (203) 432-5202. Fax: (203) 432-6144. Email: gary.brudvig@yale.edu.

‡ Current address: Graduate Group in Biophysics, University of California at San Francisco, San Francisco, CA 94143.

[1] Abbreviations: Chl, chlorophyll; Ca^{2+}-Ex-depleted PSII, PSII depleted of Ca^{2+} and the 17 and 23 kDa extrinsic polypeptides; DCBQ, 2,5-dichloro-*p*-benzoquinone; EDTA, ethylenediaminetetraacetatic acid; EXAFS, extended X-ray absorption fine structure; MES, 2-(*N*-morpholino)ethanesulfonic acid; Mn_4 cluster, oxo-bridged tetranuclear manganese cluster; OEC, oxygen-evolving complex; PSII, photosystem II; PSII membranes, photosystem II membranes which contain the 17 and 23 kDa extrinsic polypeptides; S, substrate cation which supports water oxidation; v, reaction velocity; V_M, maximum reaction velocity; Y_Z, redox-active tyrosine-161 of the D1 polypeptide.

10.1021/bi010679z CCC: $20.00
Published on Web 06/08/2001

samples to be washed of free Ca^{2+} or are performed in the steady-state. Nonetheless, there is general agreement that 1 Ca^{2+}/PSII is required for water oxidation and this Ca^{2+} is tightly bound ($K_D \sim \mu M$).

Investigating the structure of the Ca^{2+} site and its protein environment has proven to be difficult. Results from EXAFS indicate that Ca^{2+} may be quite close to the Mn_4 cluster, and Mn−Ca distances of 3.3 Å (*16, 17*) and 4.2 Å (*18*) have been reported. The latter distance is consistent with a carboxylato or halide bridge between Mn and Ca^{2+} (*1, 18*). Such a structure is supported by Fourier transform infrared absorption data that compare native and Ca^{2+}-Ex-depleted PSII (*19*), but this result is disputed (*20*). It has been shown that Ca^{2+} binding is competitive with many metal ions, including lanthanides (*21, 22*) and divalent cations such as Cd^{2+} (*23*) and Sr^{2+} (*6*), the only metal ion which functionally replaces Ca^{2+}. EPR studies of Ca^{2+}-Ex-depleted, lanthanide-substituted PSII show that the $S_1 \rightarrow S_2$ transition is blocked (*21, 24*) and that the electron transfer from Y_Z to $P680^+$ is affected (*25*). A recent $^{113}Cd^{2+}$ NMR study of Cd^{2+}-substituted PSII yielded results which suggest that the Ca^{2+} site is composed of a symmetric array of ligands including oxygen and chlorine or nitrogen atoms and may be close to the Mn_4 cluster (*26*). Illumination of Ca^{2+}-Ex-depleted PSII in the absence of competing metal ions allows the S-state cycle to advance to an intermediate step where Y_Z is oxidized with the Mn_4 cluster in the S_2 state (*7, 8, 27*). These results suggest that Ca^{2+} is intimately involved in water oxidation, possibly by participating in the organization of a hydrogen-bonding network in the OEC in all S states and binding one of the substrate water molecules necessary for O_2 formation (*1, 28*).

To date, Ca^{2+} has usually been implicated in maintaining the structure of the OEC by stabilizing the Mn_4 cluster or organizing the local ligand environment [reviewed in (*4*)]. However, what has been shown before (*29*) and what we extend in this paper is that many multivalent metal ions bind competitively with Ca^{2+}. Several of these metals can replace Ca^{2+} in other proteins with no structural perturbations (*30, 31*), yet in PSII only Sr^{2+} yields a functional active site. One might expect that if the role of Ca^{2+} were solely structural then more metal ions with structural properties similar to Ca^{2+} would at least partially restore activity; this is not the case. Lately, proposals have been put forth which progress the role of Ca^{2+} in water oxidation from a purely structural cofactor to binding a substrate water molecule involved in nucleophilic attack on a terminal Mn(V)═O species (*1, 28*). However, this proposal alone does not explain why other metal ions which could also bind a substrate water molecule do not support activity. In this paper, we quantify the binding of a series of mono-, di-, and trivalent metal ions to the Ca^{2+} site in PSII in order to understand how metal ions bind to the Ca^{2+} site and why only Ca^{2+} and Sr^{2+} support oxygen evolution. This series significantly extends the number of cations for which detailed enzyme kinetic data have been obtained. These data enable new insights to be drawn on the nature of the Ca^{2+}-binding site and the role of Ca^{2+} in water oxidation.

Falke et al. have used the competitive binding of metal ions to divalent cation-binding sites to determine the basis of cation selectivity of the site—size vs charge—and to measure the rigidity of the coordinating array of ligands (*32*). It was found that cation-binding sites which bind Mg^{2+}, the most abundant physiological divalent metal, are charge-selective, excluding monovalent cations and relying on the relatively high concentration of Mg^{2+} in vivo to discriminate it from other divalent cations (*33*). On the other hand, Ca^{2+}-binding sites also exclude monovalent cations but are size-selective, discriminating Ca^{2+} from other divalent metal ions based on their ionic radii (*34, 35*). Charge-selective sites have flexible coordination arrays and can accept cations of various sizes equally well, while size-selective sites have rigid ligand environments that optimally fit cations of a fixed radius. Therefore, data on the affinities of a series of cations with varied charges and ionic radii can provide information on the nature of the binding site. In both types of binding sites, monovalent cations have an insufficient positive charge to overcome the net negative charge-density of the coordinating array of ligands. The resulting electrostatic repulsion between the ligands does not allow them to come together to form a binding site, and so monovalent cations bind only very weakly ($K_D \gg 1$ M) to divalent cation-binding sites.

Following this methodology, we have examined the inhibition of oxygen evolution by a series of metal ions that compete for the Ca^{2+}-binding site in PSII. Using steady-state enzyme kinetics, we have determined the K_D for the metal ions, which include mono-, di-, and trivalent cations over a large range of ionic radii. The results show that the Ca^{2+}-binding site is highly size-selective. We discuss the implications for the structure of the site and consider why only Ca^{2+} and Sr^{2+} support oxygen evolution by the OEC.

EXPERIMENTAL PROCEDURES

Protein Preparations. PSII-enriched membrane fragments were isolated from market spinach as described by Berthold et al. (*36*) with the modifications of Beck et al. (*37*) and were stored in buffer containing 20 mM MES (pH 6.0), 15 mM NaCl, and 30% ethylene glycol. All preparations were performed in the dark. The PSII membrane samples were depleted of Ca^{2+} and the 17 and 23 kDa extrinsic polypeptides according to the procedure of Kalosaka et al. (*13*) with the following additional step: after treating the PSII membranes with the calcium ionophore A23187 (20 μM) in a buffer containing 40 mM MES (pH 5.0), 1.5 M NaCl, and 1 mM EGTA, the sample was pelleted and resuspended in this buffer without any ionophore, then repelleted, and the rest of the procedure was carried out without modification. This additional step yielded Ca^{2+}-Ex-depleted samples that had lower residual activity and could regain activity to the same degree as samples not treated in this way. Results for the metal ion inhibition assays were indistinguishable between Ca^{2+}-Ex-depleted PSII prepared with and without this additional low-pH treatment. Depletion of the 17 and 23 kDa extrinsic polypeptides was confirmed by SDS−PAGE using the method of Chua (*38*) with the modifications of Ikeuchi et al. (*39*) on a 12.5% (w/v) acrylamide resolving gel. The gel was stained with Coomassie Blue R-250, and densitometry scans were obtained with a Bio-Rad Scanning Densitometer (model 1650). Typically, Ca^{2+}-Ex-depleted PSII samples retained less than 5% of the 17 and 23 kDa polypeptides and greater than 95% of the 33 kDa extrinsic polypeptide. Chl concentration assays were performed using the method of Arnon (*40*).

Activity Measurements. O_2-evolution activities were measured with a Clark-type electrode at 25 °C using an Oriel 1000 W (model 66187) tungsten lamp fitted with a water filter (Oriel 6123), a 610 nm cutoff filter (Oriel LP610), and a heat filter (Schott KG5). All samples were allowed to equilibrate at room temperature for 15−20 min before being assayed. Typical O_2-evolution rates were 400−600 μmol of O_2 (mg of Chl)$^{-1}$ h^{-1} for native PSII membranes in buffer containing 20 mM MES (pH 6.0), 15 mM NaCl, 20 mM $CaCl_2$, 250 μM DCBQ, and 1 mM $K_3Fe(CN)_6$. For assays without Ca^{2+}, 40 mM $N(CH_3)_4Cl$ was used to maintain a constant [Cl^-] in the absence of Ca^{2+} (*41*). After a 4 h incubation in the dark at 4 °C, typical rates of O_2 evolution for Ca^{2+}-Ex-depleted PSII samples were 5−10% of the activity for PSII membranes and could be reconstituted to 80−90% of native activity after the addition of 20 mM $CaCl_2$, followed by another 4 h incubation. To measure the time required for a Ca^{2+}-containing, Ex-depleted PSII sample to equilibrate with a buffer lacking Ca^{2+}, PSII membranes were depleted of Ca^{2+} and the 17 and 23 kDa extrinsic polypeptides as described above. This sample was incubated in a buffer containing 20 mM MES (pH 6.0), 15 mM NaCl, 30% ethylene glycol, and 10 mM $CaCl_2$ at a [Chl] = 1 mg/mL. After 12 h, the sample was diluted 133-fold into O_2-assay buffer lacking Ca^{2+} (described above), and activity measurements were done over time.

Preparation of Inhibitor-Treated Samples. Ca^{2+}-Ex-depleted PSII samples for inhibition assays with di- and trivalent metal ions were prepared in a buffer containing 20 mM MES (pH 6.0), 15 mM NaCl, 250 μM DCBQ, and 1 mM $K_3Fe(CN)_6$ to which were added Ca^{2+} and the metal ion inhibitor from stock solutions of their chloride salts. Samples for inhibition assays with monovalent cations were prepared by omitting NaCl from the buffer described above and adjusting the pH with triethylamine rather than NaOH. Control assays with Ca^{2+}-Ex-depleted PSII in Ca^{2+}-containing buffer (as described above) demonstrated that triethylamine has no effect on O_2 evolution. The [Cl^-] was adjusted with $N(CH_3)_4Cl$ for all samples. Samples were incubated in the dark at 4 °C for at least 4 h and equilibrated at room temperature for 15−20 min before performing the assays. All samples were incubated at concentrations appropriate for oxygen assays, so no dilutions were required prior to conducting the assays.

Measurement of K_D and Calculation of Free Energy of Binding. The type of inhibition displayed by each metal ion was determined by double-reciprocal (activity^{-1} vs [Ca^{2+}]$^{-1}$) and Dixon (activity^{-1} vs [I]) plots. K_D for inhibiting cations was determined from the Dixon plots by a global linear least-squares fit of the data, constrained to intersect at a point. K_D for the activating cations Ca^{2+} and Sr^{2+} was measured by fitting a plot of activity vs [S] to the Michaelis−Menten equation:

$$\frac{v}{V_M} = \frac{[S]}{K_D + [S]} \quad (1)$$

Standard deviations were calculated by plotting the goodness-of-fit of the least-squares fits as a function of K_D (ranging from 0.5 to 1.5 times the optimal K_D) and fitting the resulting curve to a Gaussian; the full width at half-maximum of the Gaussian is reported as the standard deviation. The free energy of binding of the metal ions is defined to be

$$\Delta G_B = RT \ln K_D \quad (2)$$

as in Falke et al. (*33*). As these authors point out, using molar concentrations rather than activities makes only a small difference in the calculated free energy.

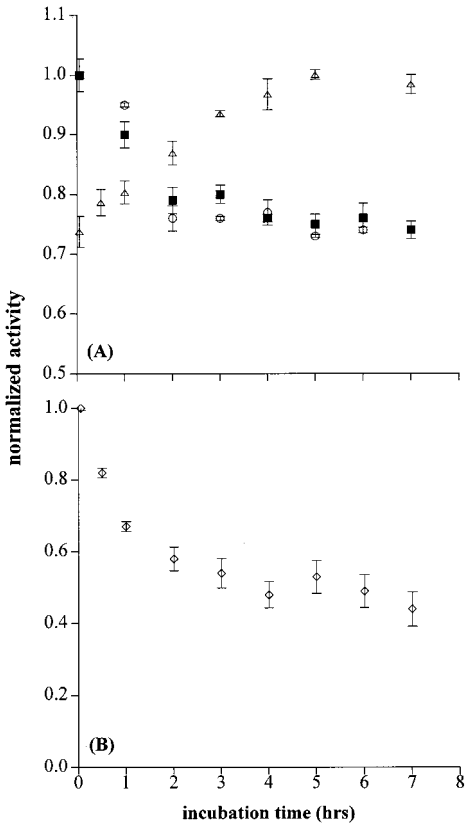

FIGURE 1: Time-course of equilibrium for inhibition and reconstitution of activity. (A) The inhibition of native (filled squares) and Ca^{2+}-Ex-depleted (open circles) PSII membranes incubated with 4 mM Ca^{2+} and 0.3 mM Gd^{3+} shows that equilibrium is reached after about 4 h. This is mirrored by the reconstitution of a Ca^{2+}-Ex-depleted PSII sample inhibited by treatment with 0.3 mM Gd^{3+} in the presence of 2 mM Ca^{2+}. This sample was incubated for 4 h, after which the Ca^{2+} concentration was increased to 8 mM by the addition of Ca^{2+} from a concentrated stock solution, and then activity measurements were conducted over time (open triangles). (B) Loss of Ca^{2+} from Ca^{2+}-containing Ex-depleted PSII (open diamonds) also requires more than 4 h to reach equilibrium. A Ca^{2+}-Ex-depleted sample was treated with 10 mM Ca^{2+} for 12 h and then diluted into Ca^{2+}-free buffer before taking activity measurements. Buffer conditions and sample preparations are described in the text. Error bars represent one standard deviation from the average of at least three trials.

RESULTS

Time-Course of Equilibrium and Reconstitution of Activity. To determine the length of incubation time required for a sample to reach equilibrium with the added metal ions, we measured the activity as a function of time at a constant inhibitor concentration (Figure 1A). All samples were prepared and incubated under the conditions required for the oxygen assays, so no sample dilutions or sudden changes of the concentrations of any of the constituents were required. Both PSII membranes and Ca^{2+}-Ex-depleted PSII membranes treated with 0.3 mM Gd^{3+} and 4 mM Ca^{2+} took 4 h to reach equilibrium. The same amount of time was required for an

Table 1: Inhibition Constants and Free Energy of Binding for Metal Ion Inhibitors of PSII

metal ion	radius (Å)[a]	pK_a aquo ion[b]	K_D (μM)[c]	ΔG_B (kcal/mol)[c]
Mg^{2+}	0.66	11.41	2840 ± 195[d]	-2.11 ± 0.14[d]
Ni^{2+}	0.69	9.86	1690 ± 192[d]	-2.42 ± 0.27[d]
Cu^{2+}	0.72	8.00	932 ± 65.6[d]	-2.77 ± 0.19[d]
Co^{2+}	0.72	9.85	1110 ± 75.5[d]	-2.66 ± 0.18[d]
Cd^{2+}	0.97	9.00	144 ± 16.0	-3.87 ± 0.43
Ca^{2+}	0.99	12.80	69.2 ± 6.61	-4.31 ± 0.41
Sr^{2+}	1.12	13.18	172 ± 9.49	-3.77 ± 0.21
Ba^{2+}	1.34	13.36	NC[f]	0
Lu^{3+}	0.85	7.94	560 ± 42.5[e]	
			(82.1 ± 17.5)	
Dy^{3+}	0.91	8.10	118 ± 9.15	-3.99 ± 0.31
			(72.0 ± 6.81)	(-5.65 ± 0.53)
Gd^{3+}	0.92	9.78	111 ± 8.91	-4.03 ± 0.33
			(79.5 ± 8.52)	(-5.59 ± 0.60)
Pr^{3+}	1.01	8.91	83.8 ± 8.26	-4.19 ± 0.41
			(27.2 ± 2.86)	(-6.22 ± 0.66)
La^{3+}	1.02	8.82	67.2 ± 5.86	-4.33 ± 0.38
			(28.7 ± 5.86)	(-6.19 ± 1.26)
Na^{+}	0.97	14.77	$\gg 1$ M	
K^{+}	1.33	16	NE[g]	
Cs^{+}	1.67	>17	NE	

[a] Data from ref (*61*). [b] Data from ref (*62*). [c] The entries are for Ca^{2+}-Ex-depleted PSII; numbers in parentheses are for PSII membranes. [d] Small contribution from mixed inhibition. [e] Mixed inhibition. [f] NC: noncompetitive. [g] NE: no effect.

inhibited sample to regain activity. To demonstrate this, a Ca^{2+}-Ex-depleted PSII sample was treated with 0.3 mM Gd^{3+} and 2 mM Ca^{2+} and incubated for 4 h, after which the [Ca^{2+}] was increased to 8 mM by the addition of Ca^{2+} from a concentrated stock solution. The subsequent increase of activity reached a constant value in 4 h. The requirement for a minimum 4 h incubation of the sample in the presence of Ca^{2+} and the inhibitor is in agreement with results obtained for Ca^{2+} binding measured by scintillation counting of $^{45}Ca^{2+}$ (*14*). It was shown in that report that several hours are required for Ca^{2+} to be incorporated into Ca^{2+}-Ex-depleted PSII under conditions similar to the ones we employed. We found that samples incubated less than 4 h yielded values of K_D that increased as the incubation time was decreased. Furthermore, the type of inhibition in these samples appeared to be mixed-competitive in cases where it was found to be pure-competitive after a 4 h incubation.

To measure the equilibration of a Ca^{2+}-containing, Ex-depleted PSII sample with a buffer lacking Ca^{2+}, a Ca^{2+}-Ex-depleted PSII sample was treated with 10 mM Ca^{2+} for 12 h. This sample was then diluted 133-fold into a buffer that lacked Ca^{2+}, and the activity was measured over time. Again, it took more than 4 h for the activity to decrease to a constant value (Figure 1B). This means that, even in the absence of the 17 and 23 kDa extrinsic polypeptides, Ca^{2+} is slow to dissociate from its binding site. Note that the final [Ca^{2+}] in the sample is approximately equal to the K_D of Ca^{2+} (Table 1), and so it would be expected that at equilibrium approximately 50% of the Ca^{2+}-binding sites should be occupied. This is confirmed by the observation that the activity reaches a constant value which is ~50% of the initial activity. On the other hand, Ca^{2+}-Ex-depleted PSII regains activity quickly when assayed with high concentrations of Ca^{2+}, which means that the association rate of Ca^{2+} must be fast. Using values of K_D from Table 1 and estimating the dissociation rate constant for Ca^{2+} from Figure 1B yield an association rate constant of 3 M^{-1} s^{-1}.

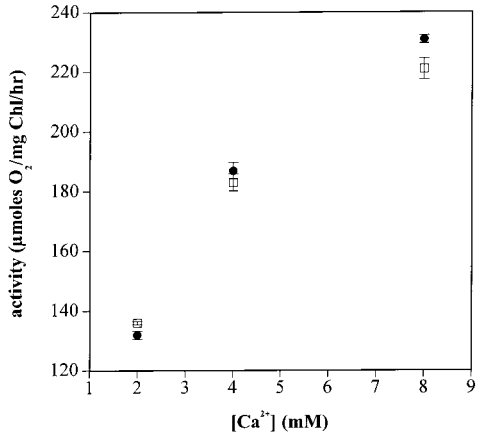

FIGURE 2: Reconstitution of activity in an inhibited Ca^{2+}-Ex-depleted PSII sample. Open squares: Activities of three separate Ca^{2+}-Ex-depleted PSII samples incubated for 4 h in the presence of 0.25 mM Dy^{3+} and 2, 4, and 8 mM Ca^{2+}. Filled circles: Reconstitution of activity of a single Ca^{2+}-Ex-depleted PSII sample initially incubated for 4 h with 0.25 mM Dy^{3+} and 2 mM Ca^{2+}. The [Ca^{2+}] of this sample was increased stepwise to 4 and 8 mM Ca^{2+} by the addition of Ca^{2+} from a concentrated stock solution. Samples were incubated for 4 h at each of the higher Ca^{2+} concentrations before the activity assays were done. Error bars represent one standard deviation from the average of at least three trials.

Our results are somewhat contrary to those obtained by Ono (*22*), who found that inhibition of Ca^{2+} binding by other metal ions was mixed-competitive and yielded very different values of K_D for a given metal ion to those we have obtained. However, in that study the sample was allowed to incubate in the presence of Ca^{2+} and the inhibitor for only 1 min, and based on our results, it is unlikely that these samples were at equilibrium before the activity measurements were performed. Our results are in better agreement with studies that found that lanthanides do bind at the Ca^{2+}-binding site in a purely competitive manner (*21*).

It is important to confirm that the inhibition of oxygen evolution by metal ions is reversible and not caused by damage to the protein. This was demonstrated by comparing the reconstitution of activity of an inhibited sample, to which Ca^{2+} was titrated back in, with the activities of different samples inhibited at fixed [Ca^{2+}]. The results are shown in Figure 2. The open squares are the activities of three separate samples of Ca^{2+}-Ex-depleted PSII incubated with 0.25 mM Dy^{3+} in the presence of 2, 4, and 8 mM Ca^{2+}. The filled circles are the activities of a single sample of Ca^{2+}-Ex-depleted PSII treated with 0.25 mM Dy^{3+} initially incubated with 2 mM Ca^{2+}. The [Ca^{2+}] was subsequently increased to 4 mM and then 8 mM, and the activities were measured after 4 h incubation in each case. That the activity of this sample increased to match those incubated at the higher fixed [Ca^{2+}] indicates that the inhibition is reversible under these conditions.

Binding of Metal Ions to the Ca^{2+} Site. The binding affinities of metal ions to the Ca^{2+} site were determined either by steady-state inhibition assays for metal ions that inhibit oxygen evolution or by titrations for metal ions which support activity. The results are summarized in Table 1. A typical example of the inhibition displayed by the di- and trivalent

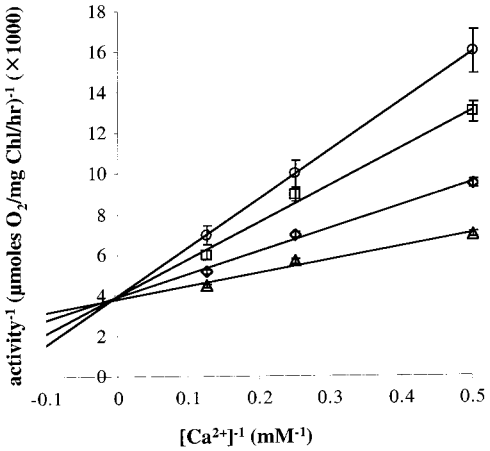

FIGURE 3: Representative double-reciprocal plot of activity^{-1} vs $[Ca^{2+}]^{-1}$ for the inhibition of Ca^{2+}-Ex-depleted PSII by 0.25 mM (open triangles), 0.5 mM (open diamonds), 0.75 mM (open squares), and 1 mM (open circles) Dy^{3+}. Error bars represent one standard deviation from the average of at least three trials.

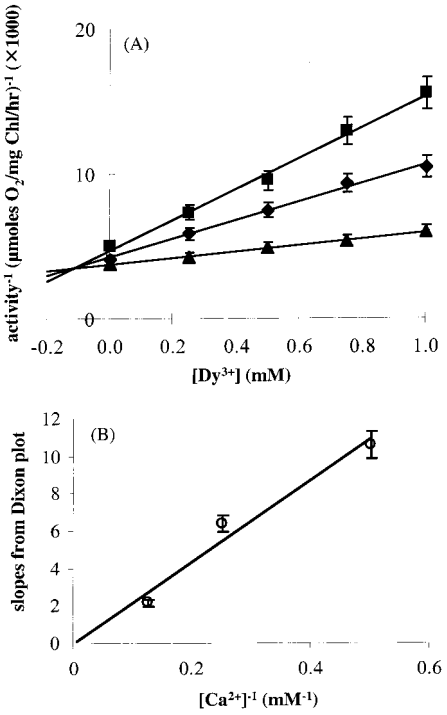

FIGURE 4: (A) Representative Dixon plot of activity^{-1} vs [I] for Ca^{2+}-Ex-depleted PSII treated with 2 mM (filled squares), 4 mM (closed diamonds), and 8 mM (closed triangles) Ca^{2+} in competition with Dy^{3+}. (B) Plot of the slopes of the lines from the Dixon plot vs $[Ca^{2+}]^{-1}$. Error bars represent one standard deviation from the average of at least three trials.

metals is illustrated by the double-reciprocal plot in Figure 3. Shown is the competition between Ca^{2+} and Dy^{3+}; the lines of best fit obtained by the global linear least-squares fitting intersect on the ordinate axis, indicating that the inhibition is competitive. This is confirmed by the Dixon plot shown in Figure 4. The lines of best fit intersect at a point in the second quadrant, and a plot of the slopes of these lines vs $[Ca^{2+}]^{-1}$ passes through the origin, indicative of competitive inhibition (*42*).

Monovalent metal ions were found to have very little or no effect on O_2 evolution, even at very high (molar) concentrations. Na^+ has an ionic radius that is very close to that of Ca^{2+}, yet it is not an inhibitor, indicating that

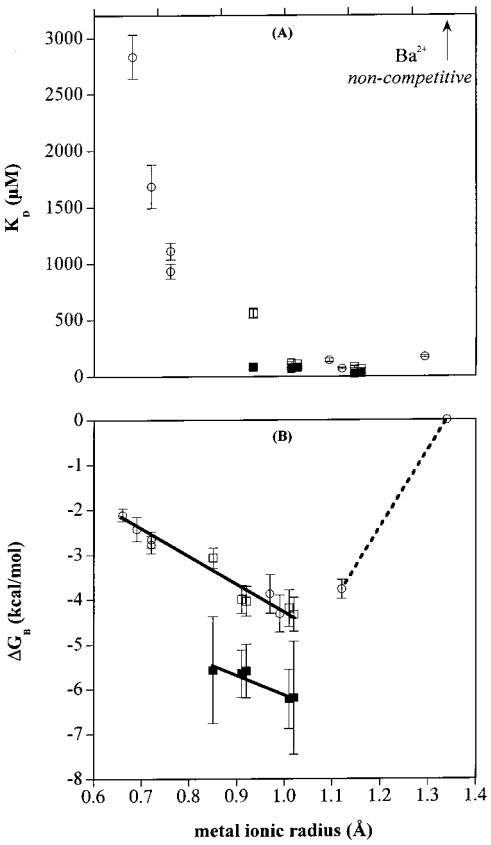

FIGURE 5: (A) K_D of the metal ions vs their ionic radius for PSII membranes treated with trivalent metals (closed squares) and Ca^{2+}-Ex-depleted PSII treated with divalent (open circles) and trivalent (open squares) metals. Ba^{2+}, a noncompetitive inhibitor which does not bind to the Ca^{2+} site, is indicated to illustrate the upper limit of the binding-site size. (B) The free energy of binding, ΔG_B, as a function of the ionic radius of the metals (symbols as above). The dashed line indicates that there is insufficient data to adequately describe the binding curve at radii larger than the optimum cavity size because metal ions with these radii are not available. Error bars represent one standard deviation from the average of at least three trials.

monovalent cations are excluded from the Ca^{2+}-binding site based on charge rather than size. It is important that divalent cation-binding sites in proteins have evolved to exclude monovalent cations, as physiological concentrations of monovalent metal ions are usually much greater than those of divalent metal ions. Our results are in disagreement with those obtained by Waggoner et al. (*41*), who found that monovalent metal ions are weak inhibitors of Ca^{2+} binding. Although the conditions under which the samples were prepared for the inhibition studies, e.g., incubation time or sample dilutions, are not stated explicitly, we suspect that these or similar differences in protocol may account for the discrepancy between our findings.

Di- and trivalent metal ions smaller than the radius of Ba^{2+} (1.34 Å) but larger than Lu^{3+} (0.85 Å) were pure competitive inhibitors. Those smaller than Lu^{3+} had a small component of mixed inhibition in Ca^{2+}-Ex-depleted PSII samples, determined from the axis intercepts of the binding curves in the double-reciprocal and Dixon plots. Figure 5A depicts the measured K_D as a function of the ionic radii of the metal ions. The K_D reaches a minimum value near the ionic radius of Ca^{2+}. This size-selectivity is better illustrated in Figure 5B, which shows ΔG_B as a function of the ionic radii of the

metal ions. Here, the turning point of the potential well for the Ca^{2+}-Ex-depleted PSII samples more clearly defines the optimal radius of the binding cavity. While for EF-hand-like Ca^{2+}-binding sites it is possible to discern the slightly more favorable ΔG_B of trivalent metal ions over divalent ones (due to more complete neutralization of the negative charge density of the ligand array) (*34*), this difference was not observed for the Ca^{2+}-binding site in PSII. Nonetheless, the Ca^{2+} site in PSII behaves very similarly to Ca^{2+}-binding sites of other proteins.

Effect of the 17 and 23 kDa Extrinsic Polypeptides on ΔG_B. Also investigated was the difference in ΔG_B between native and Ca^{2+}-Ex-depleted PSII membranes. For PSII membranes, it was only possible to collect data for metal ions with radii larger than that of Lu^{3+} (0.85 Å). Smaller metal ions had a large contribution from mixed inhibition, reflected by an intersection of the curves in a double-reciprocal plot off of the ordinate axis and a nonzero intercept in a plot of the slopes of the Dixon plots versus $[Ca^{2+}]^{-1}$ (see Figures 3 and 4). Therefore, the data for Mg^{2+}, Ni^{2+}, Cu^{2+}, and Co^{2+} inhibition of PSII membranes could not be equitably included with the rest of the data. We postulate that the origin of the mixed inhibition in PSII samples containing the 17 and 23 kDa polypeptides may be due to Ca^{2+} binding in low-affinity Ca^{2+} sites provided by these proteins. A comparison of the data in Figure 5 for native and Ca^{2+}-Ex-depleted PSII membranes shows that the presence of the 17 and 23 kDa extrinsic polypeptides enhances ΔG_B of the metals by about 2.5 kcal/mol, independent of the metal ion.

DISCUSSION

The Ca^{2+}-binding site in PSII generally behaves like many Ca^{2+}-binding sites in other proteins (*33*, *34*, *45*). Two main factors determine the selectivity of the Ca^{2+}-binding site in PSII: the size of the binding cavity and the negative charge density of the ligand array. The latter functions to exclude monovalent metal ions from the site. The mechanism for this discrimination is thought to be the electrostatic repulsion among the negatively charged carboxylate oxygens that typically comprise the coordinating array for Ca^{2+}-binding sites (*32*). Monovalent cations are insufficiently charged to overcome the negative charge density of the coordination sphere, and so the binding site does not attain a stable, closely packed cavity. Such selectivity is demonstrated by complexes of small organic ligands such as $EDTA^{4-}$, which binds monovalent ions much more weakly than di- and trivalent metal ions (*43*).

With monovalents thus excluded from the binding site, the protein must discriminate among the available multivalent cations. This is achieved by size-selectivity, as illustrated in Figure 5. A deep potential well in the plot of ΔG_B versus radius indicates strong size-selectivity, while sites that are flexible exhibit a shallow or flat trend (*32*). The divalent cation with the most favorable ΔG_B is Ca^{2+}, which lies very near the bottom of the potential well. All other divalent cations bind less tightly as their size deviates from that of Ca^{2+}. Trivalent metals ions with ionic radii comparable to that of Ca^{2+} bind equally as well, or better, than Ca^{2+}; however, as trivalent cations are scarce in vivo, the binding site would not need to have developed such a rigid array as to exclude them.

In EF-hand-like sites, it is possible to discriminate between the binding curves of di- and trivalent cations (*32*). Trivalent cations bind more tightly in EF-hand-like sites because they can more completely neutralize the negative charge-density of the ligand array. Structural differences between EF-hand sites and the OEC may explain why such discrimination is not observed in PSII. In EF-hand sites, the metal ion binding cavity is buried in a hydrophobic protein interior around which no other ions or water molecules bind. The ligand array and the charge of the metal ion are the primary factors that govern ΔG_B for a given metal ion. However, the protein environment of the OEC contains water and other ions besides Ca^{2+}. The reorganization of water dipoles and the presence of charges originating from the other cofactors could influence the charge density of the Ca^{2+}-binding site such that di- and trivalent ions bind with similar affinity. Also, it is possible that the trivalent metal ions, which are strong Lewis acids, bind with a OH^- ligand, and so have a net +2 charge upon binding.

The bottom of the potential well, which defines the optimal size of the metal ion, is not as sharp for the Ca^{2+}-binding site in PSII as it is in EF-hand sites (*32*). This suggests that there is some small amount of fluxional freedom in the binding cavity for metal ions near the optimal size. EF-hand sites have their coordination environments completely comprised of amino acid side chains which are packed tightly to form the ligand array. However, in PSII it is likely that the Ca^{2+} ion is coordinated by at least one water molecule (*44*). The mobility of a ligand such as water, which is exchangeable, possibly flexible because its orientation is not dictated by the protein backbone, and is not sterically bulky, would allow the Ca^{2+} site in PSII to be slightly less rigid than those found in EF-hand proteins. Indeed, the greater ΔG_B of EF-hand sites compared to PSII suggests this (*32*).

The steepness of the potential well at radii greater than the optimal radius defines the constraining force of the binding cavity, or the amount of work required to expand the cavity beyond its optimal size. The upper limit of the well in the large ion limit was defined to be the ionic radius of Ba^{2+}, which is a noncompetitive inhibitor and so does not bind in the Ca^{2+} site ($\Delta G_B = 0$). (It was not possible to include more data points in the large ion limit due to the lack of stable di- and trivalent metal ions in that size range, so the upper limit may actually be smaller than the ionic radius of Ba^{2+}.) The typical constraining force arising from packing forces in the interior of a protein is less than 1 kcal mol^{-1} $Å^{-1}$ (*45*); the constraining force of the Ca^{2+}-binding site in PSII is 17 kcal mol^{-1} $Å^{-1}$, similar to that measured for EF-hand-like sites (*32*). Hence, the binding site will not easily deform. This prevents the negatively charged ligand array from expanding, which would allow larger ions to occupy the site. The site is therefore highly optimized to bind metal ions of a particular size.

The potential well is less steep for ions smaller than the optimal radius, but there is still a 2-fold difference in the free energy of binding between the least and most tightly binding metals. While smaller ions such as Mg^{2+} are capable of fitting in the binding cavity, their small size does not allow optimal coordination between the metal ion and the coordinating ligands. In these cases, the hydration shell of the solvated ion provides a superior coordination environment (*33*, *35*). Figure 6 shows the free energy of binding as a

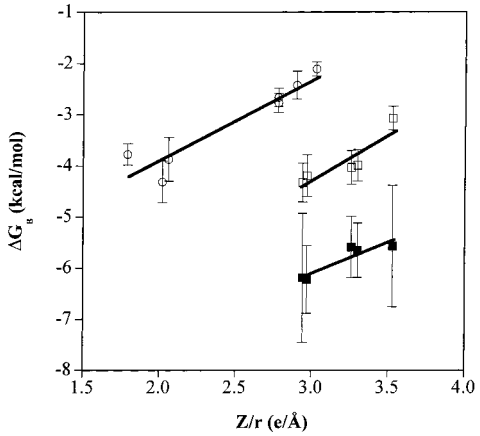

FIGURE 6: Dependence of binding free energy on the charge-to-radius ratio, an indirect measure of the dehydration free energy of the metal ions, for PSII membranes treated with trivalent metals (closed squares) and Ca^{2+}-Ex-depleted PSII treated with divalent (open circles) and trivalent (open squares) metals. The binding free energy follows the same trend within each series; the metal ions with the smallest *Z*/*r* are the easiest to dehydrate and so contribute more to the binding free energy. Error bars represent one standard deviation from the average of at least three trials.

function of the charge-to-radius ratio, a measure of the dehydration free energy for a metal ion (*46*). Metal ions with small ionic radii are more difficult to dehydrate than large metal ions. Within each series of metal ions for a given PSII sample, ΔG_B improves as *Z*/*r* decreases, i.e., as the ionic radius increases. Therefore, it is energetically more favorable for small metal ions to remain hydrated than to bind to the protein.

Comparing the results for native and Ca^{2+}-Ex-depleted PSII membranes in Figure 5 shows that the presence of the 17 and 23 kDa extrinsic polypeptides improves ΔG_B by 2.5 kcal/mol. Similar effects are observed in other Ca^{2+}-binding proteins, as well. For example, it has been shown that calmodulin undergoes conformational changes when complexed with target polypeptides that change the affinity for Ca^{2+} (*47*). The changes in ΔG_B measured for calmodulin binding to a number of peptides were slightly larger than in PSII with and without the 17 and 23 kDa extrinsic polypeptides. The energy difference in PSII is small, less than the value of a hydrogen bond, and so it is unlikely that the extrinsic polypeptides have a significant structural effect on the Ca^{2+}-binding site. We attribute the weaker binding of the metal ions in the absence of the 17 and 23 kDa extrinsic polypeptides to an increase in the local effective dielectric in the vicinity of the OEC. In the absence of the extrinsic polypeptides, bulk water approaches the lumenal surface of PSII much more closely. An increase in the local dielectric will partially screen the electrostatic interactions that govern cation binding in the Ca^{2+}-binding site. Furthermore, it seems unlikely that the extrinsic polypeptides serve as a significant diffusion barrier to Ca^{2+} exchange in dark-adapted samples because we and others (*14*) demonstrate that, even in Ex-depleted PSII membranes, it takes 4 h for Ca^{2+} to equilibrate with the bulk medium in the dark (Figure 1B). The purpose of the extrinsic polypeptides does not seem to be to prevent equilibration of Ca^{2+} with the bulk medium, but rather to increase the affinity of the Ca^{2+} site, probably by providing a low-dielectric environment in the vicinity of the OEC. The reason Ex-depleted PSII samples typically have very low activities can be attributed to Ca^{2+} loss during the course of the sample preparation, typically done in buffers which lack Ca^{2+}, and not because the removal of the extrinsic polypeptides has allowed Ca^{2+} to dissociate quickly. Furthermore, the observation that a Ca^{2+} requirement is not normally observed in PSII membrane samples unless the 17 and 23 kDa polypeptides are depleted can be explained by the change in the site affinity relative to typical background levels of Ca^{2+}. These background concentrations are in the low micromolar range based on residual Ca^{2+} in buffer reagents, which is of the same magnitude as the value of K_D for Ca^{2+} in PSII membranes but less than that for Ca^{2+} in Ex-depleted PSII membranes. The slow release of Ca^{2+} from PSII agrees with the behavior shown by the sort of Ca^{2+}-binding proteins that PSII resembles, such as EF-hand-type sites (*32*). Ca^{2+} binding in these proteins is under thermodynamic control by sites that are slow to dissociate the metal ion. This is in contrast to Ca^{2+}-binding sites in Ca^{2+}-signaling proteins, which are kinetically controlled to equilibrate with the bulk medium quickly as local Ca^{2+} concentrations rapidly change.

Overall, the affinity of cations for the Ca^{2+}-binding site in PSII is very similar to those found in other proteins (*31*, *32*). The site utilizes a high negative charge density to exclude monovalent cations from binding. The ligand sphere is quite rigid and discriminates among multivalent metal ions based on their ionic radius, with the optimal radius being that of Ca^{2+} (0.99 Å). By analogy to other Ca^{2+}-binding proteins, this suggests that the Ca^{2+}-binding site in PSII consists of an ordered closely packed array of mostly carboxylate oxygen ligands. The coordination geometry is likely to be pentagonal−bipyramidal, possibly with one or two water ligands (or another Lewis base) in place of protein residues, as is commonly the case in Ca^{2+}-binding proteins (*31*).

Considering the large number of metal ions that will compete for the Ca^{2+}-binding site in PSII, it is surprising that only Ca^{2+} and Sr^{2+} support O_2 evolution. For example, Cd^{2+} (0.97 Å) is almost the same size as Ca^{2+} (0.99 Å), carries the same charge, is a closed-shell ion, and binds with high affinity. Cd^{2+} replaces Ca^{2+} in other proteins without large structural perturbations and even preserves hydrogen-bonding networks (*30*, *31*). In the case of concanavalin A, Cd^{2+} will restore activity (*48*), yet it does not support activity in PSII. What is the distinguishing factor among the metal ions that determines functional competence in PSII?

Several proposals assign a structural role for Ca^{2+} in PSII, such as maintaining the structural stability of the Mn_4 cluster (*49*). Ca^{2+} has been implicated in organizing the ligand environment of the OEC, similar to the structural role played by Zn^{2+} in Cu/Zn superoxide dismutase (*50*). It has also been suggested that Ca^{2+} participates in conformational changes (*8*) and pK_a shifts of carboxylate groups (*51*) during S-state advancement. Ca^{2+} has been assigned the role of the docking site for Cl^- so that the availability of Cl^- is not rate-limiting during S-state cycling (*52*, *53*). These proposals suggest that structural factors should determine whether a metal ion can functionally replace Ca^{2+} in PSII. However, we can rule out a purely structural role for Ca^{2+} based on the results of our metal ion binding studies. Many of the metal ions investigated in this study have a preferred geometry but still bind quite well in a rigid binding site optimized for a spherical

metal ion, so it is unlikely that the coordination geometry of the ligand sphere is distorted. If geometry were important, the site would not display the rigid size selectivity for multivalent metal ions, but would reject those metals that are not compatible with the ligand geometry of the site. Furthermore, based on the argument made above for Cd^{2+}, it remains unclear why the requirement for Ca^{2+} is so strict, allowing only Sr^{2+} to reconstitute activity.

Recently, a few groups have put forth proposals in which Ca^{2+} plays a direct role in water oxidation chemistry. In the model of Pecoraro et al., a terminal Mn(V)═O species undergoes a nucleophilic attack by a Ca^{2+}-bound hydroxide ligand to form a Mn-bound hydroperoxide (*28*). Density functional theory calculations conducted by Siegbahn (*54*) in which Ca^{2+} is directly bridged to the Mn_4 cluster by μ-OH or μ-O ligands suggest that Ca^{2+} is required to form an oxygen radical in the S_3 state. Our group proposed that Ca^{2+} binds a substrate water molecule and tunes its reactivity for nucleophilic attack on a terminal Mn(V)═O species (*1*).

We postulate that Ca^{2+} plays an active role in water oxidation and can only be substituted by Sr^{2+} because the electronegativity of the two metal ions is similar, which is directly related to their Lewis acidity and hence the pK_a of their water ligands (*55*). The function of Ca^{2+} as a Lewis acid is to tune the Brønsted acid−base properties of a coordinated water molecule that either is involved in a proton-coupled electron-transfer pathway and/or is a substrate in O_2 formation. Other metal ions fail to support oxygen evolution because their Lewis acidity is too far out of the range required for activity (Table 1), which makes the coordinated water too strong of a Brønsted acid. The result is that either the hydrogen-bonding network of the OEC is disturbed or the coordinated water deprotonates to form OH^-. This idea is similar to one proposed by Penner-Hahn and co-workers to explain why the 2.7 Å distance attributed to Mn−Mn scattering in EXAFS spectra of PSII was sensitive to the replacement of Ca^{2+} by Dy^{3+} (*56*). The observations were explained by a model in which a Ca^{2+}-bound water molecule forms a hydrogen bond with a μ-oxo bridge between two Mn ions. Because Dy^{3+} is a much stronger Lewis acid than Ca^{2+}, water bound to Dy^{3+} is a stronger Brønsted acid and may protonate the bridging μ-oxo, thus changing the Mn−Mn distance. Protonation of the μ-oxo bridge would also be expected to change the reduction potential of the Mn_4 cluster (*57*) that may prevent its oxidation by $Y_Z^\bullet$ in Dy^{3+}-substituted PSII.

In our model of the OEC (*1*), a substrate water molecule bound to Ca^{2+} forms a hydrogen bond to a bridging μ-oxo of the Mn_4 cluster, as proposed by Penner-Hahn and co-workers (*56*). Oxidation of the Mn_4 cluster via proton-coupled electron transfer leads to the formation of a Mn(V)═O species in the S_4 state that undergoes a nucleophilic attack by the Ca-bound water molecule. This would transiently form a Mn(III)-OOH moiety which releases O_2 following reduction of the Mn_4 cluster. There are two possibilities for the protonation state of the electrophilic Ca^{2+}-bound water, either OH^- or H_2O. When buried in the hydrophobic interior of a protein, the pK_a of water bound to a metal ion is usually lowered several units; nonetheless, the relative ordering of the Lewis acidity of the metal ions in Table 1 will remain the same. Taking this into consideration, the Ca^{2+} aqua ion is still a weak Lewis acid (pK_a = 12.8) compared to the other metal ions in Table 1, and so we propose that H_2O, and not OH^-, is the form of the Ca^{2+}-bound substrate molecule. Sr^{2+} is the only other catalytically competent metal ion because its pK_a is sufficiently high that it provides H_2O and not OH^- as a ligand.

In a recent paper, Babcock and co-workers showed that substitution of Sr^{2+} for Ca^{2+} results in a slowing of the reduction of $Y_Z^\bullet$ (*58*). These authors argue that if Ca^{2+} were involved directly in water oxidation, then only the O−O bond-forming step should be affected by Sr^{2+} substitution and not any prior S-state advances. They conclude that small disturbances within the OEC lead to the slowing of $Y_Z^\bullet$ through an increase in the activation barrier for proton-coupled electron transfer. However, this argument does not preclude Ca^{2+} from having a direct role in water oxidation in addition to having an effect on the structure of the OEC. If Ca^{2+} binds close to the Mn_4 cluster, as is thought (*16*−*18*), then Ca^{2+} will necessarily have an effect on the structure of the OEC. The primary role of Ca^{2+} in water oxidation is not structural, however, or any divalent cation of the appropriate size would support activity. Rather, the strict requirement for Ca^{2+} or Sr^{2+} appears to be related to a physical characteristic of the metal ions, their Lewis acidity.

All of the other metal ions in Table 1 that compete for the Ca^{2+}-binding site would, in our model, be sufficiently strong Lewis acids that they would provide OH^- rather than H_2O as a ligand. The inhibition of water oxidation by these metal ions could possibly be due to protonation of basic sites within the OEC, as proposed by Penner-Hahn (*56*), or because OH^- is not a viable substrate. For example, Babcock and co-workers have argued that attack of OH^- on a Mn(V)═O species may not be favorable due to the slight negative charge of the metal−oxo moiety (*59*), which would electrostatically repel OH^- and significantly increase the activation energy of O−O bond formation (*60*). In addition, protonation of basic groups in the OEC or simply lack of two protons on the Ca^{2+}-bound water may disrupt the hydrogen-bonding network and prevent proton-coupled electron transfer leading to S-state advancement.

In conclusion, we found that the Ca^{2+}-binding site in PSII is composed of a rigid array of ligands that discriminates Ca^{2+} from other physiological metal ions based on size and charge. The low dielectric of the site is maintained by the 17 and 23 kDa extrinsic polypeptides, which increases the binding affinity of cations for the site. Given that so many divalent cations bind competitively in the Ca^{2+}-binding site, but only Ca^{2+} and Sr^{2+} restore activity, we propose that the role of Ca^{2+} in PSII is chemical rather than purely structural. We present a model for the participation of Ca^{2+} in water oxidation in which Ca^{2+} acts as a Lewis acid and binds a substrate water molecule that undergoes nucleophilic attack on a Mn(V)═O species in O−O bond formation. Other cations inhibit water oxidation by promoting the deprotonation of this water molecule to form OH^-, which may not be a viable substrate, or by disrupting the hydrogen-bonding network in the OEC and retarding proton-coupled electron transfer. This proposal can be tested by examining the effect of pH on the activity of metal ion-substituted PSII. We are currently conducting experiments to investigate the pH dependence of oxygen evolution in PSII samples treated with various metal ions.

ACKNOWLEDGMENT

We thank Dr. Henriette A. Kühne for her assistance with the global linear least-squares fitting of the data. We are very grateful to Susy Kohout for useful comments and discussions.

REFERENCES

1. Vrettos, J. S., Limburg, J., and Brudvig, G. W. (2001) *Biochim. Biophys. Acta 1503*, 229−245.
2. Yachandra, V. K., Sauer, K., and Klein, M. P. (1996) *Chem. Rev. 96*, 2927−2950.
3. Britt, R. D. (1996) in *Oxygenic Photosynthesis: The Light Reactions* (Ort, D. R., and Yocum, C. F., Eds.) pp 137−159, Kluwer Academic Publishers, Dordrecht, The Netherlands.
4. Debus, R. J. (1992) *Biochim. Biophys. Acta 1102*, 269−352.
5. Brand, J. J., and Becker, D. W. (1984) *J. Bioenerg. Biomembr. 16*, 239−249.
6. Ghanotakis, D. F., Babcock, G. T., and Yocum, C. F. (1984) *FEBS Lett. 167*, 127−130.
7. Boussac, A., Zimmermann, J.-L., and Rutherford, A. W. (1989) *Biochemistry 28*, 8984−8989.
8. Boussac, A., Zimmermann, J.-L., and Rutherford, A. W. (1990) *FEBS Lett. 277*, 69−74.
9. Ghanotakis, D. F., Topper, J. N., Babcock, G. T., and Yocum, C. F. (1984) *FEBS Lett. 170*, 169−173.
10. Miyao, M., and Murata, N. (1984) *FEBS Lett. 168*, 118−120.
11. Nakatani, H. Y. (1984) *Biochem. Biophys. Res. Commun. 120*, 299−304.
12. Han, K.-C., and Katoh, S. (1995) *Biochim. Biophys. Acta 1232*, 230−236.
13. Kalosaka, K., Beck, W. F., Brudvig, G. W., and Cheniae, G. (1990) in *Current Research in Photosynthesis* (Baltscheffsky, M., Ed.) pp 721−724, Kluwer, Dordrecht, The Netherlands.
14. Ädelroth, P., Lindberg, K., and Andréasson, L.-E. (1995) *Biochemistry 34*, 9021−9027.
15. Grove, G., and Brudvig, G. W. (1998) *Biochemistry 37*, 1532−1539.
16. Cinco, R. M., Robblee, J. H., Rompel, A., Fernandez, C., Yachandra, V. K., Sauer, K., and Klein, M. P. (1998) *J. Phys. Chem. B 102*, 8248−8256.
17. Latimer, M. J., DeRose, V. J., Yachandra, V. K., Sauer, K., and Klein, M. P. (1998) *J. Phys. Chem. B 102*, 8257−8265.
18. Penner-Hahn, J. E., Fronko, R. M., Pecoraro, V. L., Yocum, C. F., Betts, S. D., and Bowlby, N. R. (1990) *J. Am. Chem. Soc. 112*, 2549−2557.
19. Noguchi, T., Ono, T., and Inoue, Y. (1995) *Biochim. Biophys. Acta 1228*, 189−200.
20. Smith, J. C., Gonzalez, V. E., and Vincent, J. B. (1997) *Inorg. Chim. Acta 255*, 99−103.
21. Ghanotakis, D. F., Babcock, G. T., and Yocum, C. F. (1985) *Biochim. Biophys. Acta 809*, 173−180.
22. Ono, T. (2000) *J. Inorg. Biochem. 82*, 85−91.
23. Waggoner, C. M., and Yocum, C. F. (1990) in *Current Research in Photosynthesis* (Baltscheffsky, M., Ed.) pp 733−736, Kluwer, Dordrecht, The Netherlands.
24. Bakou, A., Buser, C., Dandulakis, G., Brudvig, G., and Ghanotakis, D. F. (1992) *Biochim. Biophys. Acta 1099*, 131−136.
25. Bakou, A., and Ghanotakis, D. F. (1992) *Biochim. Biophys. Acta 1141*, 303−308.
26. Matysik, J., Alia, Nachtegaal, G., van Gorkom, H. J., Hoff, A. J., and de Groot, H. J. M. (2000) *Biochemistry 39*, 6751−6755.
27. Hallahan, B. J., Nugent, J. H. A., Warden, J. T., and Evans, M. C. W. (1992) *Biochemistry 31*, 4562−4573.
28. Pecoraro, V. L., Baldwin, M. J., Caudle, M. T., Hsieh, W.-Y., and Law, N. A. (1998) *Pure Appl. Chem. 70*, 925−929.
29. Yocum, C. F. (1992) in *Manganese Redox Enzymes* (Pecoraro, V. L., Ed.) pp 71−83, VCH, New York.
30. Bouckaert, J., Loris, R., and Wyns, L. (2000) *Acta Crystallogr. D56*, 1569−1576.
31. McPhalen, C. A., Strynadka, N. C. J., and James, M. N. G. (1991) *Adv. Protein Chem. 42*, 77−144.
32. Falke, J. J., Drake, S. K., Hazard, A. L., and Peersen, O. B. (1994) *Q. Rev. Biophys. 27*, 219−290.
33. Needham, J. V., Chen, T. Y., and Falke, J. J. (1993) *Biochemistry 32*, 3363−3367.
34. Snyder, E. E., Buoscio, B. W., and Falke, J. J. (1990) *Biochemistry 29*, 3927−3943.
35. Falke, J. J., Snyder, E. E., Thatcher, K. C., and Voertler, C. S. (1991) *Biochemistry 30*, 8690−8697.
36. Berthold, D. A., Babcock, G. T., and Yocum, C. F. (1981) *FEBS Lett. 134*, 231−234.
37. Beck, W. F., de Paula, J. C., and Brudvig, G. W. (1985) *Biochemistry 24*, 3035−3043.
38. Chua, N.-H. (1980) *Methods Enzymol. 69*, 434−446.
39. Ikeuchi, M., Yuasa, M., and Inoue, Y. (1985) *FEBS Lett. 185*, 316−322.
40. Arnon, D. I. (1949) *Plant Physiol. 24*, 1−15.
41. Waggoner, C. M., Pecoraro, V., and Yocum, C. F. (1989) *FEBS Lett. 244*, 237−240.
42. Segel, I. H. (1975) *Enzyme Kinetics*, John Wiley & Sons, New York.
43. Christensen, J. J., Eatough, D. J., and Izatt, R. M. (1975) *Handbook of Metal Ligand Heats and Related Thermodynamic Quantities*, Marcel Dekker, New York.
44. Hillier, W., and Wydrzynski, T. (2001) *Biochim. Biophys. Acta 1503*, 197−209.
45. Sandberg, W. S., and Terwilliger, T. C. (1991) *Trends Biotechnol. 9*, 59−63.
46. Rashin, A. A., and Honig, B. (1985) *J. Phys. Chem. 89*, 5588−5593.
47. Peersen, O. B., Madsen, T. S., and Falke, J. J. (1997) *Protein Sci. 6*, 794−807.
48. Pandolfino, E. R., Christie, D. J., Munske, G. R., Fry, J., and Magnuson, J. A. (1980) *J. Biol. Chem. 255*, 8772−8775.
49. Ghanotakis, D. F., and Yocum, C. F. (1990) *Annu. Rev. Plant Physiol. Plant Mol. Biol. 41*, 255−276.
50. Yocum, C. F. (1991) *Biochim. Biophys. Acta 1059*, 1−15.
51. Boussac, A., and Rutherford, A. W. (1988) *FEBS Lett. 236*, 432−436.
52. Hoganson, C. W., and Babcock, G. T. (1997) *Science 277*, 1953−1956.
53. Tommos, C., and Babcock, G. T. (1998) *Acc. Chem. Res. 31*, 18−25.
54. Siegbahn, P. E. M. (2000) *Inorg. Chem. 39*, 2923−2935.
55. Brown, I. D., and Skowron, A. (1990) *J. Am. Chem. Soc. 112*, 3401−3403.
56. Riggs-Gelasco, P. J., Mei, R., Ghanotakis, D. F., Yocum, C. F., and Penner-Hahn, J. E. (1996) *J. Am. Chem. Soc. 118*, 2400−2410.
57. Manchanda, R., Thorp, H. H., Brudvig, G. W., and Crabtree, R. H. (1992) *Inorg. Chem. 31*, 4040−4041.
58. Westphal, K. L., Lydakis-Simantiris, K., Cukier, R. I., and Babcock, G. T. (2000) *Biochemistry 39*, 16220−16229.
59. Blomberg, M. R. A., Siegbahn, P. E. M., Styring, S., Babcock, G. T., Åkermark, B., and Korall, P. (1997) *J. Am. Chem. Soc. 119*, 8285−8292.
60. Siegbahn, P. E. M., and Crabtree, R. H. (1999) *J. Am. Chem. Soc. 121*, 117−127.
61. Weast, R. C. (1978) in *CRC Handbook of Chemistry and Physics* (Weast, R. C., Ed.) CRC Press, West Palm Beach, FL.
62. Dean, J. A. (1985) in *Lange's Handbook of Chemistry* (Dean, J. A., Ed.) McGraw-Hill Book Co., New York.

BI010679Z